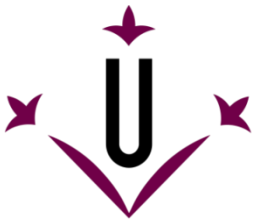

Growth, wood anatomy and stable isotopes shows species-specific couplings in three Mexican conifers inhabiting drought-prone areas

Arturo Pacheco[1*], J. Julio Camarero[2], Marín Pompa-García[3], Giovanna Battipaglia[4], Jordi Voltas[5,6], Marco Carrer[1]

[1*]Universitá degli Studi di Padova, Dip. TeSAF, I-35020 Legnaro, Italy
[2]Instituto Pirenaico de Ecología (IPE-CSIC). Avda. Montañana 1005, Apdo. 202, E-50192 Zaragoza, Spain.
[3]University of Juarez del Estado de Durango, faculty of forest sciences, Rıo Papaloapan y Blvd. Durango S/N Col. Valle del Sur, CP 34120 Durango, Mexico.
[4]University of Campania 'L. Vanvitelli', Department of Environmental, Biological and Pharmaceutical Sciences and Technologies, via Vivaldi 43, I-81100 Caserta, Italy.
[5] Joint Research Unit CTFC - AGROTECNIO, Av. Alcalde Rovira Roure 191, 25198 Lleida, Spain.
[6] Department of Crop and Forest Sciences, Universitat de Lleida, Av. Alcalde Rovira Roure 191, 25198 Lleida, Spain

*Corresponding author:
Arturo Pacheco Solana
Universitá degli Studi di Padova
Dip. TeSAF
I-35020 Legnaro, Italy
E-mail: arturo.pachecosolana@phd.unipd.it

KEYWORDS: dendroecology, wood anatomy, drought stress, conifers, dendroanatomy, Mexico, Sierra Madre Occidental, water-use efficiency

RUNNING HEAD: Growth, wood anatomy and isotopes of conifers in a climate gradient of Mexico

ABSTRACT

An improved understanding of how tree species will respond to warmer conditions and longer droughts requires comparing their responses across different environmental settings and considering a multi-proxy approach. We used several traits (tree-ring width, formation of intra-annual density fluctuations –IADFs, wood anatomy, $\Delta^{13}C$ and $\delta^{18}O$ records) to retrospectively quantify these responses in three conifers inhabiting drought-prone areas in northwestern Mexico. A fir species (*Abies durangensis*) was studied in a higher altitude and slightly rainier site and two pine species were sampled in a nearby, lower drier site (*Pinus engelmannii*, *Pinus cembroides*). Tree-ring-width indices (TRWi) of the studied species showed a very similar year-to-year variability likely indicating a common climatic signal. Wood anatomy analyses done over 3.5 million measured cells and showed that *P. cembroides* lumen area was much smaller than in the other two species and it remained constant along all the studied period (over 64 years). Instead, cell wall thickness was widest in *P. engelmannii* and this species presented the highest amount of intra-annual density fluctuations. Climate and wood anatomy correlations pointed out that lumen area was positively affected by winter precipitation for all studied species, while cell-wall thickness was negatively affected by this season's precipitation in all species but *P. cembroides*. Stable isotope analysis showed significantly lower values of $\Delta^{13}C$ for *P. cembroides* and no significant $\delta^{18}O$ differences between the three species, although they shared a common decreasing trend. With very distinct wood anatomical traits (smaller cells, compact morphology), *P. cembroides* stood out as the better adapted species in its current environment and could be less affected by future drier climate. *P. engelmannii* and *A. durangensis* showed high plasticity at wood anatomical level, allowing them to promptly respond to seasonal water availability but likely gives few advantages on future climate scenarios with longer and frequent drought spells.

1. INTRODUCTION

Global warming projections indicate a mean temperature increase of 1.5 ºC above pre-industrial levels in the forthcoming 30 years (IPCC, 2018). Accordingly, the increment in the frequency and intensity of dry spells and heat waves will progressively constrain forest growth and productivity, especially in drought-prone areas (IPCC, 2013; Vicente-Serrano et al., 2013). Climate models for Southwest USA and Northwest Mexico line up with the aforementioned predictions of increasing aridification and long-term water shortage in this dry area where the summer Monsoon represents the major source of rainfall to mountain conifer forests (Cook and Seager, 2013; Williams et al., 2013).

Mexican mountains contain 43% of the world's pine species, and half of these occur at the Sierra Madre Occidental mountain range in the northwestern part of the country (Sánchez-González, 2008). The geographic extension of this range (1,200 km) and its position between the Pacific Ocean and the semi-arid Mexican plateau results in climatic gradients which likely allowed the occurrence of endemic conifers like *Abies durangensis* Martínez on the higher wet sites or *Pinus cembroides* Zucc. on the dry lower areas (Gernandt and la Rosa, 2014; González-Elizondo et al., 2012). Besides its ecological value and environmental services, the mixed conifer forests of the Sierra Madre Occidental provide direct economic resources throughout timber, lumber, cones, wildlife hunting and cattle raising to the inhabitants of this region (Fulé et al., 2011).

In mountain terrain, climatic gradients due to elevation difference and rain shadow effects can be used to understand the species responses to local conditions and the consequences of global warming at a regional scale (Fritts, 1974; Van de Water et al., 2002). Trees growing at lower elevations and drier sites of the southwest USA and northern Mexico are potentially more affected by drought than those located at higher altitude where mesic conditions prevail (Adams and Kolb 2005, Kelly and Goulden 2008, McDowell et al. 2010, González-Cásares

et al. 2017). However, conifer species growing at higher elevation (*Abies durangensis*, *Picea chihuahuana*) have been shown to be more vulnerable to drought spells than those from lower and more xeric conditions (*Pinus engelmannii* Carr, *Pinus cembroides*), in which much longer drought periods are needed to provoke negative impacts in the trees (Pompa-García et al. 2017a, 2017b). Furthermore, it has also been reported that, in other sites under semi-arid conditions like Northern Arizona (Adams and Kolb, 2005), the Colorado Plateau (Salzer and Kipfmueller, 2005) and Northeastern Mexico (Villanueva-Diaz et al., 2007), previous winter precipitation is more tightly correlated with radial growth (positively) than any other precipitation period during the growth season. This effect of winter precipitation on growth has been detected by performing climate-growth correlations using tree rings (total width or earlywood width) in United States and Mexico. Recent studies conducted in e.g. Northeastern Spain (Pacheco et al., 2018, 2016) demonstrated the importance of using a multidisciplinary approach involving, in particular, wood anatomical features (e.g. cell lumen area, cell wall thickness) and tree-ring isotope analyses (De Micco et al., 2019). This approach allowed obtaining valuable intra-annual resolution of these climate-growth relations and therefore to better infer the most responsive growth period to rainy conditions, but it also provided a closer view on the functional aspects of plant-environment interactions (Castagneri et al., 2017; Fonti et al., 2010).

Water limitation causes a vast array of responses in trees, including the reduction of stomata conductance and photosynthetic rate which trigger changes in isotope fractionation depending on CO_2 uptake and fixation. The final result of these cascading effects is the differences of isotope composition of the tree's tissues (Battipaglia et al. 2010, Granda et al. 2014). Specifically, carbon isotope composition ($\delta^{13}C$) reflects changes in gas exchange, with less negative values corresponding to improved water-use efficiency (Saurer et al., 2004), whereas oxygen isotope composition ($\delta^{18}O$) is correlated with soil water sources and stomatal

conductance rates, thus responding to evaporative demand (Saurer et al., 1997). Therefore, tree rings can be used to get retrospective multi-species information on drought effects by analyzing stable isotope signatures along with radial growth (Shestakova et al., 2017). It is important, however, to take into account that tree-ring isotope ratios merge information on xylem cells formed during different periods of the year, which could cause offset problems when trying to precisely match pattern and process (Porté and Loustau, 2001).

In this study, we analyzed three endemic conifers growing on a climatic gradient at the Sierra Madre in Northwestern Mexico: *Abies durangensis*, *Pinus engelmannii* and *Pinus cembroides*. The aim of our research is to integrate growth, wood anatomy and isotope records to quantify how these species respond to climate variability, especially drought, and to forecast how they may react to ongoing climatic change. Although previous multi-taxa studies have been conducted in this area at locations with contrasting water availability (González-Cásares et al., 2017; Herrera-soto and Gonz, 2018; Pompa-García et al., 2017a, 2017b), they agree on the need of further research considering complementary high-detailed methodologies. This is the first study performed in Northwestern Mexico combining the traditional tree-ring approach with state-of-the-art wood anatomy analysis and $\delta^{13}C$ and $\delta^{18}O$ information.

2. MATERIALS AND METHODS

2.1 Study area, climate and tree species

This study was conducted in two sites (wet and dry) located on an ecologically valuable mountain forest region in the Sierra Madre Occidental (Durango state, northern Mexico), considered as a hotspot of biodiversity that comprises ecologically valuable mixed conifer forest (Aguirre et al., 2003). For the wet site (23.63º N, 105.38º W) we selected an area located near the town of El Salto at an altitude of around 2700 m a.s.l., which registers a

mean annual temperature (MAT) of 10.7 ºC and a mean annual precipitation (MAP) of 939 mm (Supporting Information, Fig. S1). For the dry site (24.06º N, 105.02º W) sampling was performed at an altitude of 2200 m a.s.l. presenting a MAT of 12.6 ºC and a MAP of 673 mm, close to the town of Otinapa (Table 1). Both sites are characterized by a pine forest mixed with other conifers where selection management has been done in the past. The selected species are all native of northwest Mexico. From Otinapa, these are *Pinus engelmannii* and *Pinus cembroides*, and from El Salto *Abies durangensis*. These species have been previously used for tree-ring research primarily focusing on the reconstruction of hydro-climatic conditions and on the analysis of drought sensitivity and tolerance (Bickford et al., 2011; Constante García et al., 2009; González-Cásares et al., 2017; Pompa-García et al., 2017b, 2017a; Villanueva-Diaz et al., 2007; Villanueva-Díaz et al., 2014).

We obtained monthly climate data (mean temperature, total precipiation) from the two stations. We also calculated the Standardized Precipitation Evapotranspiration Index (SPEI), a multi-scalar drought index, using these data and following Vicente-Serrano et al. (2010).

Table 1. Features of the three sampled conifers in the wet and dry sites. DBH is the diameter measured at breast height (1.3 m); TRW is the tree-ring width; EPS is the Expressed Population Signal. Values are means ± SE. Tree-ring descriptive statistics correspond to the common period 1950-2014.

Site	Site type	Species	N	DBH (cm)	Height (m)	Age at 1.3 m (years)	TRW (mm)[a]	*R*bar[b]	EPS[b]
El Salto	Wet	*Abies durangensis*	15	40.5 ± 10.5	17.2 ± 4.6	80 ± 14	2.00 ± 0.22	0.29	0.89
Otinapa	Dry	*Pinus engelmannii*	14	40.0 ± 4.2	13.6 ± 1.7	79 ± 8	1.77 ± 0.17	0.30	0.90
		Pinus cembroides	12	37.1 ± 3.8	8.0 ± 0.8	139 ± 13	0.75 ± 0.09	0.58	0.96

[a] Variables calculated on raw tree-ring width data
[b] Variables calculated on ring-width indices

2.3 Field sampling and tree-ring data

During the winter of 2015, a total of 10-15 dominant trees per species were sampled and their

size was measured using tapes and a clinometer (DBH, the diameter measured at breast height, i.e. 1.3 m; total height). We took at least two radial cores per tree at 1-1.3 m with a 5-mm Pressler increment borer. One core was used for obtaining ring-width data, whereas another core was used for isotope analyses. Sampled trees were randomly selected and field sampling followed standard dendrochronological methods (Fritts, 1976). The collected wood samples were air-dried and then polished with a series of successively finer sand-paper grits until rings were clearly visible. Tree rings were measured to the nearest 0.01 mm using a binocular stereoscope and a LINTAB measuring device (Rinntech, Heidelberg, Germany). Cross-dating of the tree-ring series was checked using the program COFECHA (Holmes 1983). To remove trends and growth pulses caused by age, competition or disturbances, we calculated ring-width indices (TRWi) to quantify growth variability at inter-annual scales following the standard methodologies in dendrochronology (Cook et al., 1990). Individual series were fitted using a cubic smoothing splines function with 50% frequency–response cutoff of 30 years. Autoregressive models were then applied to remove most of the first-order temporal autocorrelation related to the previous year growth and to obtain pre-whitened or residual indices. Lastly, we calculated mean series (chronologies) of the residual indices for each species using biweight robust means. This procedure was performed using the ARSTAN program (Cook, 1985). Finally, as a way to detect changes on radial growth and forest productivity, we calculated the basal area increment (BAI) from raw tree-ring records.

2.4 Wood-anatomy analyses

A third 10-mm core was obtained from each tree for wood-anatomy analyses. The cores of the six best cross-dated trees per species were selected for this purpose. The selected cores were diagonally cut into 4-cm long pieces, boiled in water in order to soften the wood and sliced into 10-12 μm thick transversal sections using a rotary microtome (Leica RM 2025,

Heidelberg, Germany). The samples were stained with safranin (1%) and astrablue (0.5%) (both diluted in distilled water) and rinsed with water and ethanol. Afterwards they were fixed on permanent slides with Eukitt (BiOptica, Milan, Italy). Histological images where obtained using a D-sight 2.0 System automatic scanner (Menarini Diagnostics, Florence, Italy) at 100× magnification, with a resolution of 1.99 pixels μm^{-1}. Tree-ring borders were manually drawn on the images, which went through a semi-automatically analysis using the ROXAS v3 software (von Arx and Carrer, 2014). This analysis provided measurements (among others) of transversal lumen area (LA) and cell-wall thickness (CWT) of tracheids, while assigning to each measured cell its relative position within the dated annual ring. Following a partitioning method (Castagneri et al., 2018) we used the relative position of each tracheid within each ring, to calculate mean values of LA and CWT along 10 equal-width tangential sectors to obtain a very detailed profile of anatomical features changes along the whole ring. These ten sectors are assigned and named accordingly from the early earlywood (S1) to the late latewood (S10).

Intra-annual density fluctuations (IADFs) in tree rings are generally considered structural anomalies caused by deviations from the "normal course" of xylogenesis during the growing season (De Micco et al., 2016). IADFs were visually quantified and separated in two main groups (earlywood and latewood IADFs), according to the position within the ring where they were present. The earlywood IADFs are characterized as a band of latewood-like cells (i.e. tracheids with small LA and thick CWT) within the earlywood, while latewood-IADF are bands of earlywood-like cells (i.e. tracheids with large LA and thin CWT) within the latewood. Each of these groups were also visually categorized in three levels of intensity (weak, moderate and strong) according to how much the anatomic measurements of the band cells diverged from the average of those surrounding them (Supporting Information, Fig. S2).

208

209 **2.5 Isotope analysis**

210 The 5-mm cores of the six best cross-dated trees per species were selected for isotope
211 analyses. We obtained annual pools of wood for each species considering the common period
212 1980-2010. Wood samples were carefully homogenized and milled using an ultra-
213 centrifugation mill (Retsch ZM1, mesh size of 0.5 mm). Wood α-cellulose was extracted
214 following Brendel et al. (2000) and Gaudinski et al. (2005). Briefly, the extraction involves
215 soaking the wood samples in a 10:1 mixture of acetic (80 %) and nitric acid (69 %) at 120°C
216 for 45 minutes in 1.5 ml polypropylene tubes, followed by a series of rinses using ethanol,
217 deionized water and acetone. A final purification step uses 17 % w/v NaOH and subsequent
218 rinsing steps with water, acetic acid and acetone. The samples are finally left to dry overnight
219 and placed in an oven for 2 h at 50°C. An aliquot of 0.5-0.7 mg of each α-cellulose sample
220 was weighed on a balance (Mettler Toledo AX205) and placed into tin (for $\delta^{13}C$) and silver
221 (for $\delta^{18}O$) capsules, respectively.

222 The C and O stable isotope compositions were measured at the IRMS Lab of
223 University of Campania "L. Vanvitelli" by continuous-flow isotope ratio mass spectrometry
224 (Delta V plus Thermo Electron Corporation, Bremen Germany) using 0.06 mg of dry matter
225 for $\delta^{13}C$ and 0.3-0.6 mg for $\delta^{18}O$.

226 Carbon isotope discrimination ($\Delta^{13}C$; Farquhar and Richards, 1984) was calculated as:

227 $$\Delta^{13}C = (\delta^{13}C_{atm} - \delta^{13}C_{plant}) / (1+\delta^{13}C_{plant}/1000) \quad (1),$$

228 where $\delta^{13}C_{atm}$ and $\delta^{13}C_{plant}$ are the carbon isotope composition of atmospheric CO_2 and tree-
229 ring α-cellulose, respectively, expressed in parts per thousand (‰) relative to the standard V-
230 PDB; $\Delta^{13}C$ is linearly related to the ratio of intercellular (c_i) to atmospheric (c_a) CO_2 mole
231 fractions, by (Farquhar et al., 1982):

232 $$\Delta^{13}C = a + (b-a)\, c_i/c_a \quad (2),$$

where a is the fractionation during CO_2 diffusion through the stomata (4.4‰), and b is the fractionation associated with reactions by Rubisco and PEP carboxylase (27‰; Farquhar and Richards, 1984). The values for variables c_a and $\delta^{13}C_{atm}$ were obtained from published data (McCarroll and Loader, 2004).

The c_i/c_a ratio reflects the balance between net assimilation (A) rate and stomatal conductance to CO_2 (g_c) according to Fick's law: $A = g_c(c_a - c_i)$. Stomatal conductance to CO_2 and water vapor (g_w) are related by a constant factor ($g_w = 1.6g_c$), and hence these last two variables allow linking the leaf-gas exchange of carbon and water. The linear relationship between c_i/c_a and Δ may be used to estimate intrinsic water-use efficiency (iWUE), defined as the ratio of net carbon assimilation to stomatal conductance to water (A/g_w), which is calculated as follows:

$$\text{iWUE} = (c_a / 1.6)\,[(b - \Delta) / (b - a)] \quad (3)$$

The iWUE (μmol mol^{-1}) inferred from wood $\Delta^{13}C$ has been widely used to assess trends in the internal regulation of carbon uptake and water loss in trees (McCarroll and Loader, 2004), assuming that $\Delta^{13}C$ relates linearly to c_i/c_a. However, the iWUE should not be considered as equivalent to instantaneous water-use efficiency, which is the ratio of assimilation (carbon gained) to transpiration (water lost) and takes into account the atmospheric water demand (Seibt et al., 2008).

2.6 Statistical analyses

We compared mean growth, anatomy and isotope data between species using Mann-Whitney tests. Prior to analysing how climate was related to wood-anatomical traits, the individual series were detrended by a 32-year cubic smoothing spline to remove age-related growth trend. The climate-anatomy associations were quantified using Pearson correlations between the detrended wood-anatomical parameters (LA and CWT) and the monthly climatic data

(mean temperature, total precipitation) from El Salto and Otinapa weather stations covering a 60 year period (1950-2010).

Finally, we considered the three theoretical scenarios of iWUE proposed by Saurer et al. (2004): (i) constant c_i, (ii) constant c_i/c_a , and (iii) constant $c_a - c_i$. These three scenarios differ in the degree to which the increase in c_i follows the increase in c_a: (i) not at all, (ii) proportionally, or (iii) at similar rate. In scenario (i) iWUE increases strongly, while in scenario (ii) iWUE is improved, but not as strongly as in scenario (i). Finally, iWUE remains constant in scenario (iii). To assess the goodness of fit of the three iWUE theoretical models as compared to observed iWUE data we quantified the Root Mean Squared Error (RMSE), which measures the mean deviation of fitted from observed data (Chatfield 2000). The RMSE is the square root of the variance of the residuals, which is equivalent to the standard deviation of the unexplained variance, i.e. lower RMSE values correspond to a better fit.

3. RESULTS

3.1 Growth and wood anatomical traits

Tree-ring width indices (TRWi) of the studied species showed a very similar year-to-year variability, thereby indicating a common climatic signal (Figure 1). Correlations between the mean species series were always highly significant ($p < 0.0001$), with highest values between *A. durangensis* and the pine species ($r = 0.57 - 0.58$) than between both pine species ($r = 0.48$). Growth rates (BAI) for *A. durangensis* and *P. engelmannii* were significantly higher (20.06 cm^2 and 20.59 cm^2 respectively) than those of *P. cembroides* (5.48 cm^2) (Table 2). In general, *A. durangensis* showed a steadier annual growth along the studied period (CV = 33.1%), while the pine species went through more dynamic changes following consistently wet or dry periods (*P. cembroides*, CV = 36.1%, *P. engelmannii*, CV = 49.3%). Using the

common period 1950-2014 for all three species, we produced a very detailed description of wood anatomy (LA, CWT). In total, we analyzed over 3.5 million individual cells: 1.6×10^6 for *A. durangensis*, 1.3×10^6 for *P. engelmannii* and 0.8×10^6 for *P. cembroides* (Figure 2). Regarding LA, *P. cembroides* showed the smallest tracheid dimensions of all species (591.23 ± 4.92 μm^2) which remained fairly constant along the studied period (CV = 6.5%). Instead, the other two species had wider tracheids, although no significantly different between them (LA: *P. engelmannii*, 1019. 99 ± 14.60 μm^2; *A. durangensis*, 1074.83 ± 19.22 μm^2) and also presented a higher year-to-year variability (*P. engelmannii*, CV= 11.2%; *A. durangensis*, CV = 14.0%) (Table 2), but with a slightly increasing trend along the 64-year period analyzed.

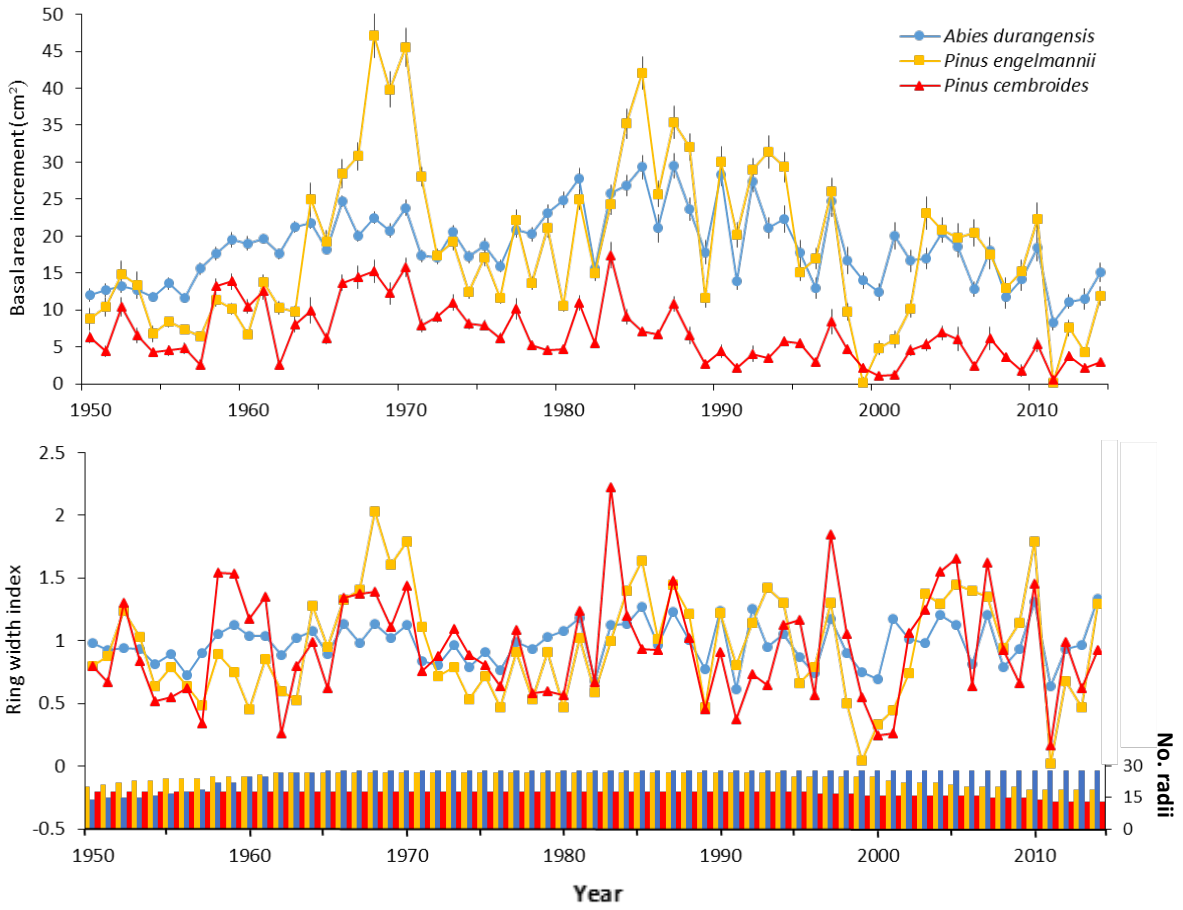

Figure 1. Basal area increment and ring-width indices of the three studied conifer species (wet site, *Abies durangensis*; dry site, *Pinus cembroides* and *Pinus engelmannii*). Data correspond to means (± SE) and include the best replicated common period from 1950-2014. Bars in the lowermost plot indicate sample depth.

The CWT analyses reveal the same trends mentioned before i.e. increasing values for *P. engelmannii* and *A. durangensis*, and a mostly flat response for *P. cembroides* (Figure 2). All three species showed a significantly different CWT, with *A. durangensis* having the thinnest (4.18 ± 0.03 µm) and *P. engelmannii* the widest cell walls (5.54 ± 0.04 µm). CWT variability was similar between species (CV =4.4-6.3%). From an intra-annual perspective *P. engelmannii* confirms its characteristically thicker cell wall along all ring width sectors, while *A. durangensis* maintains a wider lumen area on the last sectors of growth (S5 to S10) (Supporting information Fig S3).

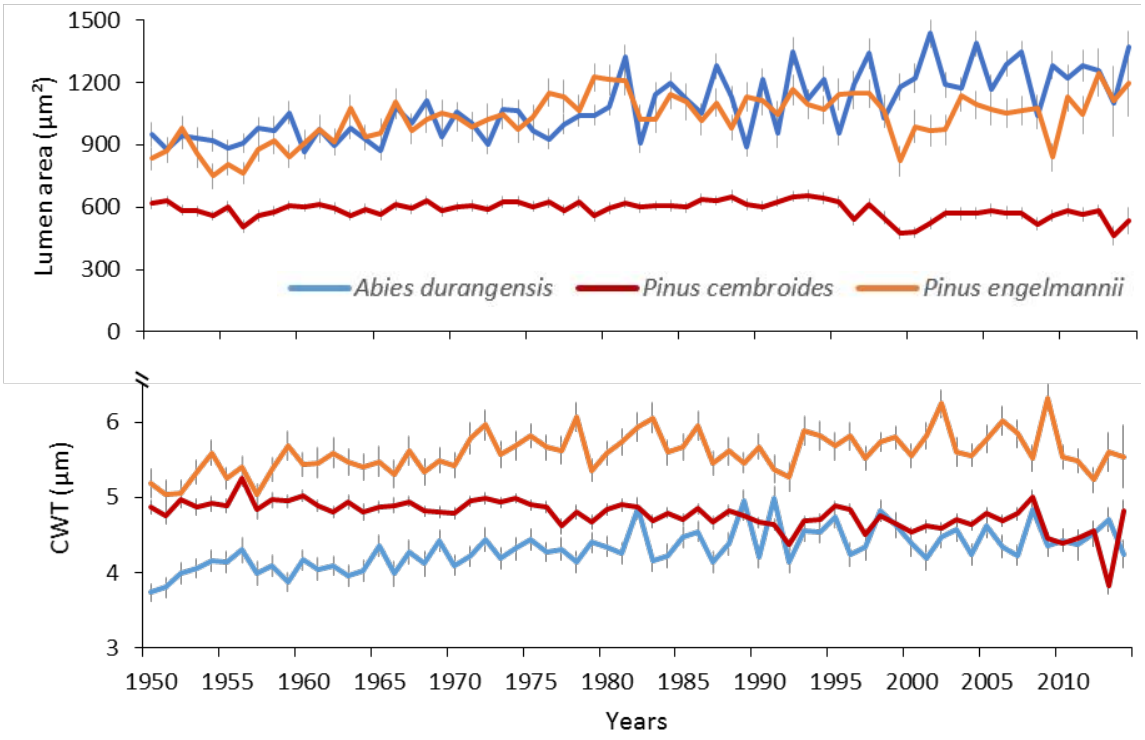

Figure 2. Non-detrended wood anatomical series (means ± SE) of lumen area and cell wall thickness (CWT) for the common period of 1950-2014 in the three studied conifer species (wet site, *Abies durangensis*; dry site, *Pinus cembroides* and *Pinus engelmannii*).

Table 2. Mean (±SE) values for the measured variables of radial growth (basal area increment), wood anatomy (lumen area, cell-wall thickness) and isotope data (cellulose-$\Delta^{13}C$; cellulose-$\delta^{18}O$; iWUE, intrinsic water-use efficiency). Reported variables correspond to the period 1980-2010. Different letters indicate significant ($p < 0.05$) differences between species (Mann-Whitney *U* tests).

Species	BAI (cm^2)	Lumen area (μm^2)	Cell-wall thickness (μm)	$\Delta^{13}C$ (‰)	$\delta^{18}O$ (‰)	iWUE ($\mu mol\ mol^{-1}$)
A. durangensis	20.06 ± 0.99b	1074.83 ± 19.22b	4.18 ± 0.03a	14.75 ± 0.11c	25.67 ± 0.15b	106.97 ± 1.27a
P. engelmannii	20.59 ± 1.77b	1019. 99 ± 14.60b	5.54 ± 0.04c	13.80 ± 0.10b	24.84 ± 0.08a	116.17 ± 1.39b
P. cembroides	5.48 ± 0.60a	591.23 ± 4.92a	4.27 ± 0.02b	12.30 ± 0.06a	24.96 ± 0.11a	131.35 ± 1.02c

3.2 Intra-annual density fluctuations

The two pine species growing at the Otinapa dry site showed a similar proportion of earlywood IADF (ew-IADF) to latewood IADF (lw-IADF), 90% to 10% respectively (Figure 3). In the case of *A. durangensis* at the El Salto wet site lw-IADF represented over 25% of all IADFs. *Pinus engelmannii* presented the highest presence of IADFs, with almost 65% of the years presenting one IADF, and followed by *A. durangensis* with around 40% of incidence, while *P. cembroides* was the least affected, with just one third of its rings showing intra-annual changes of wood density. Along all three species, the 2^{nd} to 4^{th} sectors of the ring (earlywood) presented most IADFs formation. A schematic characterization of IADFs along time (Figure 4) shows how lw-IADF on *A. durangensis* has become less common since the mid-1980s, while for the two pine species the IADF patterns have not significantly changed during the last 60 years.

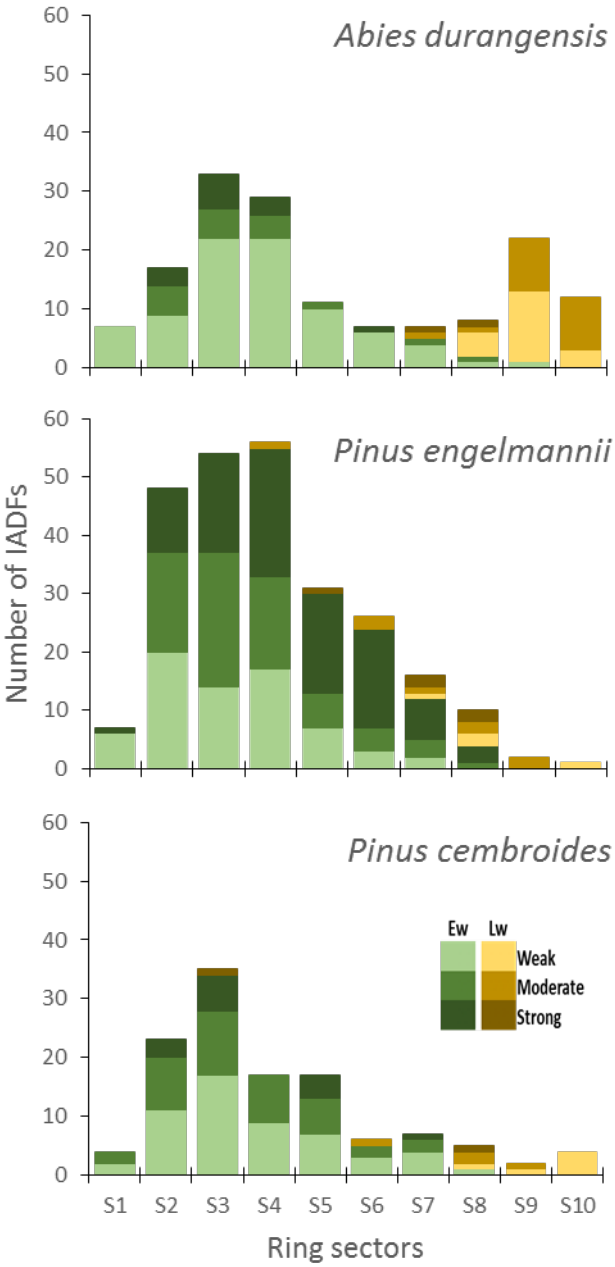

Figure 3. Quantification and characterization along the 10 tree-ring radial sectors of each intra-annual density fluctuations (IADF) present across all tree cores analyzed from the three conifer species (wet site, *Abies durangensis*; dry site, *Pinus engelmannii* and *Pinus cembroides*). This characterization is based on the location of the IADFs within the earlywood (green bars, sectors S1 to S6) or latewood (brown bars, sectors S7 to S10) areas and the intensity of its fluctuation (color tone). Quantification and characterization were performed from 1945 to 2010.

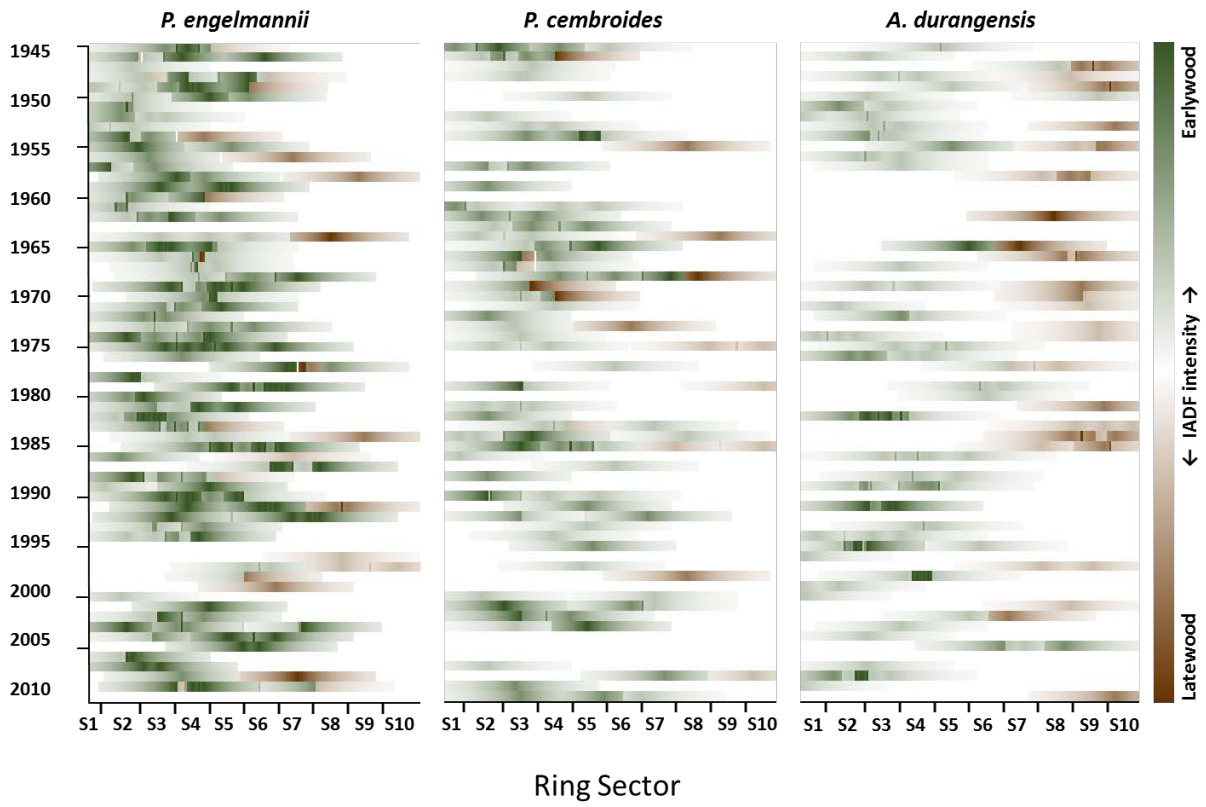

Figure 4. Quantification and characterization of each intra-annual density fluctuations (IADF) present across all tree cores analyzed from the three conifer species (wet site, *Abies durangensis*; dry site, *Pinus cembroides* and *Pinus engelmannii*) along the 10 tree-ring radial sectors (x axes; radial sectors go from the early earlywood (S1) to the late latewood (S10)) from 1945 to 2010. Characterization is based on the location of the IADF within the earlywood (greens) or latewood (browns) areas and the intensity of its fluctuation.

3.3 Stable isotopes and intrinsic water-use efficiency

The $\Delta^{13}C$ values of wood α-cellulose were significantly lower for *P. cembroides* compared to the other two species, with *A. durangensis* presenting consistently the highest values (Figure 5). When considering their intrinsic inter-annual variation, this was relatively lower for *P. cembroides* (CV = 1.2%) as compared to the other two species (CV >2.5%).

Also, $\delta^{18}O$ of wood α-cellulose did show a decreasing trend for all the species (Figure 5). There were no significant differences between the two pine species from the dry site at Otinapa, while in the case of *A. durangensis* its $\delta^{18}O$ values were significantly higher.

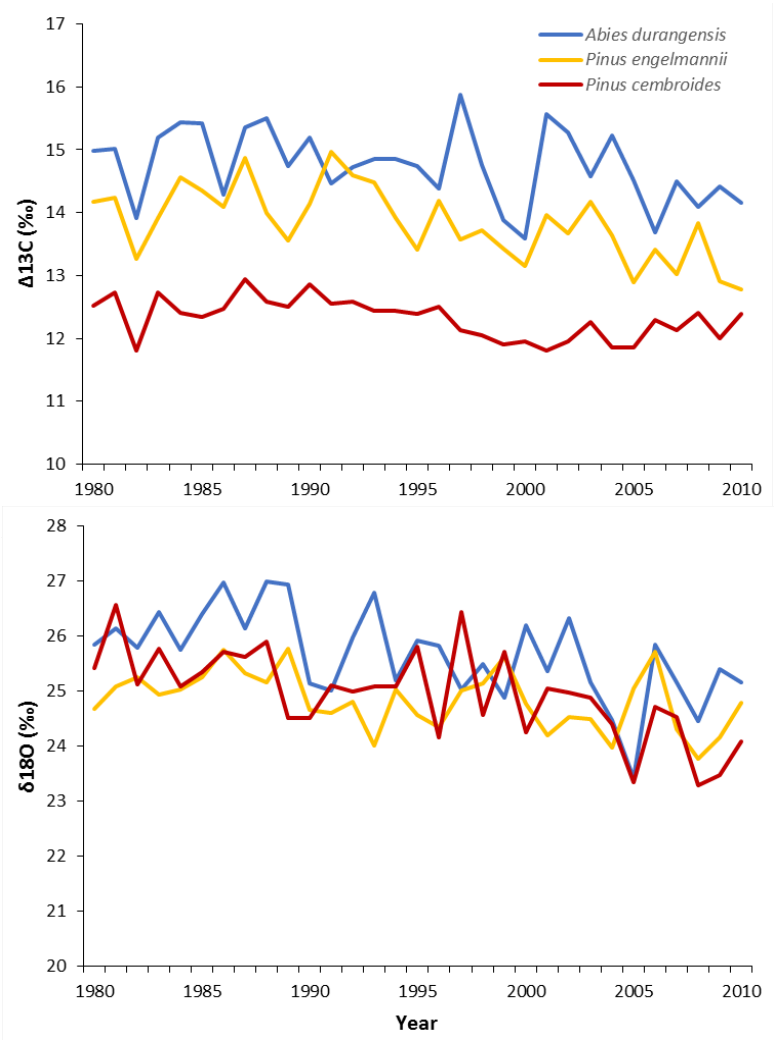

Figure 5. Variability of cellulose-$\Delta^{13}C$ and cellulose-$\delta^{18}O$ in the three conifer species (wet site, *Abies durangensis*; dry site, *Pinus cembroides* and *Pinus engelmannii*). Values are shown for the period 1980-2010.

All three species presented a sustained increase in iWUE along the studied period (Figure 6). In agreement with the $\Delta^{13}C$ analysis, *P. cembroides* had significantly higher iWUE values if compared to the other two species (Table 2). According to the iWUE scenarios, the best models (lowest RMSE) in all species corresponded to the constant c_i/c_a scenario in which iWUE is improved but not as much as in the constant c_i scenario (Table 3).

Table 3. Goodness-of-fit statistics (RMSE, root mean squared error, in μmol mol^{-1}) for the three different theoretical models of intrinsic water-use efficiency (iWUE) fitted to the iWUE data (1980-2010 period) of the three tree species (see Fig. 6). Abbreviations: c_a, atmospheric CO_2 concentration; c_i, CO_2 concentration in the internal sub-stomatal cavity of leaves.

Species	iWUE models		
	Constant c_i	Constant c_i/c_a	Constant $c_a–c_i$
A. durangensis	1.88	0.88	1.72
P. engelmannii	1.53	0.98	2.01
P. cembroides	1.56	0.48	1.74

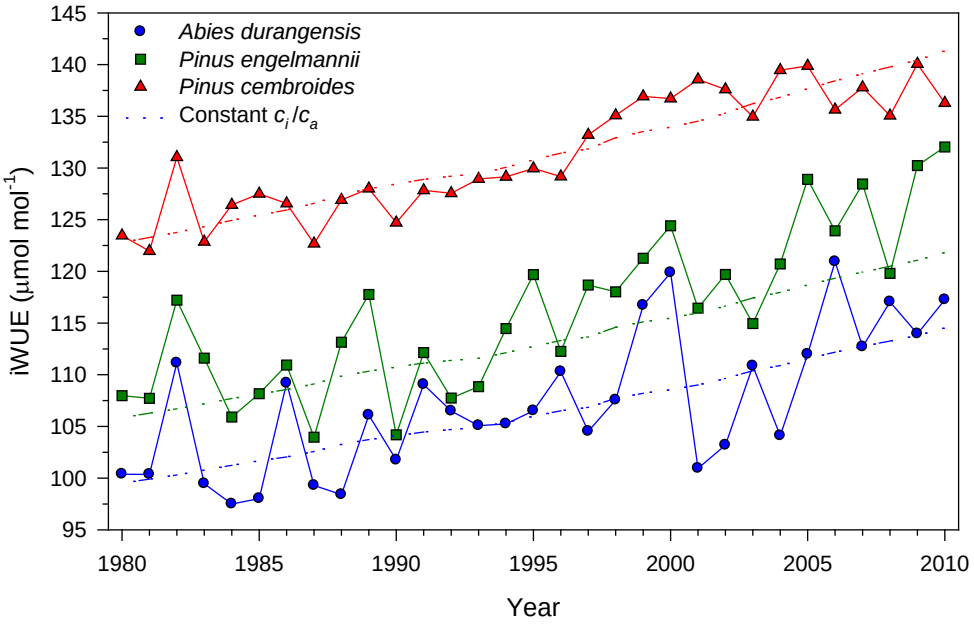

Figure 6. Trends in intrinsic water-use efficiency (iWUE) of the three species (wet site, *Abies durangensis*; dry site, *Pinus engelamannii* and *Pinus cembroides*) and selected iWUE model (constant c_i/c_a ratio, dashed lines).

3.4 Relationships between growth, wood-anatomical traits and isotope variables

A. durangensis portrayed clearly significant relationships between its growth and both wood anatomical traits (LA [positive], and CWT [negative]), whereas the two pines species showed no significant correlation between these variables (Table 4). Correlations between the two anatomical features were consistently negative for the three species, although non-significant in the case of *P. cembroides*. When analyzing the relations with isotopes, all species showed

a significant positive correlation between BAI and $\Delta^{13}C$, but when considering the anatomical traits, only *A. durangensis* had significant correlations with $\Delta^{13}C$ (positive with LA and negative with CWT). In the case of $\delta^{18}O$, only *P. cembroides* showed a significant correlation with growth (positive with BAI).

Table 4. Pearson correlations calculated by relating mean values of growth (BAI, basal area increment), wood anatomy (LA, lumen area; CWT, cell-wall thickness) and isotope data ($\Delta^{13}C$ and $\delta^{18}O$). Correlations were calculated for the common period 1980-2010. Significance levels: $*P < 0.05$, $**P < 0.01$, and $***P < 0.001$.

Species	Variable	BAI	LA	CWT	$\Delta^{13}C$
Abies durangensis	LA	0.58***			
	CWT	-0.45**	-0.85***		
	$\Delta^{13}C$	0.74***	0.43*	-0.36*	
	$\delta^{18}O$	0.27	-0.02	-0.09	0.15
Pinus engelmannii	LA	0.33			
	CWT	-0.12	-0.47**		
	$\Delta^{13}C$	0.52**	0.24	-0.27	
	$\delta^{18}O$	0.13	-0.23	0.04	0.01
Pinus cembroides	LA	0.33			
	CWT	0.30	-0.23		
	$\Delta^{13}C$	0.41*	0.32	0.06	
	$\delta^{18}O$	0.49**	0.23	0.10	0.33

3.5 Associations between wood anatomical traits and climate

All species were positively affected by winter precipitation producing larger tracheids after wet winters (i.e. bigger LA), but each site reflected this influence in different sectors along the tree ring. In the case of El Salto (wet site), *A. durangensis* showed strong associations along all tree-ring sectors, starting from S1 to S4 (earlywood), which correlated with the winter precipitation (December to February), and from S5 to S10 sectors (latewood) coinciding with spring and early summer precipitations. However, for both pine species growing in the dry site late winter precipitation showed its effects after S6 to S10 sectors (Figure 7). Regarding correlations with CWT, *A. durangensis* showed a significantly negative

correlation for most tree growth sectors in correspondence to late spring and early summer precipitation (May and June). In the case of pines, only *P.engelmannii* showed a significant negative correlation with winter precipitation (January and February), while *P. cembroides* did not show any significant correlation.

Figure 7. Climate-anatomy associations between lumen area or cell wall thickness and monthly precipitation for the two studied areas (wet site for *Abies durangensis*; dry site for *Pinus engelmannii* and *Pinus cembroides*) over the common period 1950–2014. Pearson correlations were computed

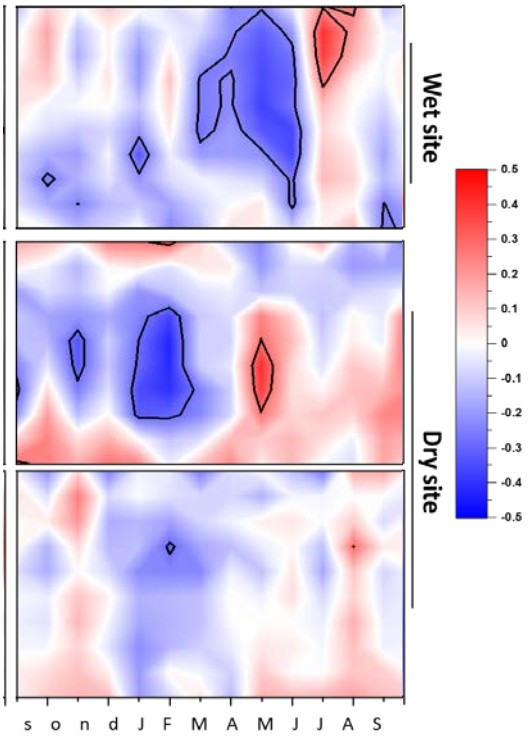

from September of the previous year (months abbreviated by lowercase letters) to September of the next year (months abbreviated by uppercase letters), and they were calculated using the ten tree-ring radial sectors from the early earlywood (S1) to the late latewood (S10) (y axes). Correlation coefficients above $|0.232|$ are significant at $p < 0.05$ and they are signaled by contour black lines.

4. DISCUSSION

This study is the first to apply classical dendrochronology, wood anatomy and isotopic analysis in Mexico to asses and compare how three conifer species cope with climatic

variability in a mountainous region of northern Mexico, a region particularly susceptible to climate change and forecasted aridification trends (Stahle et al., 2016). Across all the study period, *Pinus cembroides* was the species that consistently showed the most divergent results compared to the other species. This pine shows significantly smaller tree-ring width and cell lumen area, has the least percentage of IADFs presence and almost no climatic correlations with cell wall thickness, and displays the highest iWUE. Although *P. cembroides* trees are older than the other sampled conifers (Table 1), all species are in a mature stage and, therefore, most of the aforementioned differences can be attributed to species specific physiological characteristics. In the case of *P. cembroides* its short height and extended root system may help it to cope with the drier conditions of its habitat (Gutiérrez-García et al., 2015). Contrastingly to the other much taller studied tree species, *P. cembroides* also presents smaller lumen area, following the allometric model where conduits diameter respond to plant height (Carrer et al., 2015). Consequently, *Pinus engelmannii*, which coexists with *P. cembroides*, is almost twice its height and it presents significantly different results in most of the studied parameters, including lumen area. Its results run closer to those shown by *A. durangensis* growing in the higher and rainier site.

From a secondary growth perspective, *P. engelmannii* has a more plastic response as it presents over double the amount of IADFs (Figure 3) than its concurrent pine species. These characteristics suggest that both pines species have different strategies to withstand water shortage at the dry site. While *P. cembroides* relays on maintaining a shorter height with smaller tracheids and slower growth rates, *P. engelmannii* produce larger tracheid with thicker cell walls (Figure 2). A similar scenario was described between two coexisting conifers on northeastern Spain (Pacheco et al., 2016) where the smaller species (*Juniperus thurifera*) formed smaller cells than its concurrent larger species (*Pinus halepensis*). In our case both species are congeneric and the smaller lumen area of *P. cembroides* cells could

make its xylem less vulnerable to cavitation. Thus, this species may be better adapted to withstand drought than its coexisting pine species having wider tracheids (Willson et al., 2008). Although the thicker cell walls of *P. engelmannii* can also sign a different strategy to cope with dry weather as the tracheid's thickness-to-span ratio is considered a primary determinant of the xylem resistance to hydraulic failure by implosion (Hacke et al., 2001; Pittermann et al., 2006). Considering this characteristic *P. engelmannii*, being a much taller tree, can compete with *P. cembroides* at the dry conditions of Otinapa without risking tracheid embolism. The climate-anatomy correlations (Figure 7) provide further insight on the different wood anatomic features of these pines. While both species depend on late winter- early spring precipitation for growth and tracheid enlargement, only *P. engelmannii* shows a significant negative response for cell wall thickness, meaning that during rainy winters this species invests less on cell wall reinforcement.

At El Salto wet site, *Abies durangensis* was the species with the strongest climate-anatomy correlations. As reported in previous studies (Pompa-García et al., 2017a, 2017b), this species (and others like *Picea chihuahuana*) growing in areas with a mostly positive water balance (Figure S1) shows a higher sensitivity to weather changes (mainly drought) than other conifers inhabiting lower and drier environments. In our study, the species' precipitation-anatomy associations span along all tree-ring sectors and show a congruent succession of positive values with lumen area, followed by negative ones for cell wall thickness during the growing season (Figure 7). However, to the best of our knowledge, no xylogenesis studies have been carried out in this area (neither with these species) to confirm the genuine start and end of the growing season and, therefore, we need a better assessment of the cambial phenology in these forests to thoroughly confirm our hypothesis. It should be noted that, contrary to the pine species, *A. durangensis* shows a significant negative correlation between precipitation and CWT at the end of summer affecting only the last two sectors. This

481 particularity is clearly substantiated by the IADFs results (Figure 3) where this species is the
482 only one to produce a significant amount of latewood IADFs on the 9^{th} and 10^{th} tree-ring
483 sector. Furthermore, according to Figure 4, this behavior has become rarer on the last 30
484 years, which can be a result of the continued increase of temperatures and evapotranspiration
485 at El Salto (Pompa-García et al., 2017b). Latewood density fluctuations are commonly
486 attributed to an increase of water availability at the end of summer or during autumn
487 (Battipaglia et al., 2016; Bouriaud et al., 2005; Campelo et al., 2007; De Micco et al., 2016;
488 Novak et al., 2013; Pacheco et al., 2018). Although precipitation patterns have not changed at
489 El Salto, the aforementioned temperature increase may be reducing soil moisture and
490 increasing evaporative demand, hampering in this way the responsiveness to summer rainfall
491 pulses and the formation of latewood IADFs on the last decades. Considering the interaction
492 of these climatic factors, we also observed that *A. durangensis* cell wall thickness was
493 negatively correlated with the SPEI, while pine species were not (Supporting information Fig.
494 S4).

495 The climatic gradient on which this study has been developed cannot explain by itself
496 the high variability of these results. The species functional characteristics play a decisive role
497 on how trees respond to climate and, especially, on a changing climate scenario. The
498 projected higher temperatures and lower precipitations (IPCC2018) could produce a higher
499 interspecific competition for soil water resources (Linares et al., 2010). This new condition
500 could prove detrimental for old and tall individuals like *P. engelmannii* which can face more
501 difficulties for the uptake of water and nutrients up to the topmost parts of the crown (Singer
502 et al., 2013). Conversely, species like *P. cembroides* – with smaller size and smaller conduits
503 – could be less prone to the deterioration of their hydraulic system (Bennett et al., 2015).
504 The isotope results showed that all three species had positive and significant correlations
505 between $\Delta^{13}C$ and growth (BAI), while for the anatomical variables only *A. durangensis*

showed significant correlations (Table 4). The positive correlation found between $\Delta^{13}C$ and LA in *A. durangensis* and its correspondent negative correlation with CWT results on a riskier morphological strategy of its xylem to cope with drought conditions, demonstrating higher sensitivity to drought conditions as previously observed (Pompa-García et al., 2017a). This would put the species' at risk of conduit embolism in case of increasing dry conditions of its habitat. In the case of $\delta^{18}O$, only *P. cembroides* had a significant positive correlation with BAI, which may indicate a denser and shallower root system allowing *P. cembroides* to take advantage (in terms of growth) of small rainfall episodes which are a more isotopically enriched water source (Canadell and Zedler, 1995; Moreno-Gutiérrez et al., 2012, 2015). The $\Delta^{13}C$ series (Figure 5) of the three species showed no particular differences on their trends along the studied period. However, it is noteworthy to highlight the extremely low cellulose-$\Delta^{13}C$ values achieved by *P. cembroides*, which to the best of our knowledge are among the lowest values ever reported in the literature for a forest tree species (or the highest values of iWUE). Even for an extremely plastic and water-saving species such as *Pinus halepensis*, the observed iWUE inferred from wood α-cellulose achieved appreciably lower values under particularly dry conditions (De Micco et al., 2019). Indeed, and considering the three proposed theoretical models of intrinsic water-use efficiency (Saurer et al., 2004) (Table 3), the constant *ci/ca* scenario was the best describing the rising trend of *P. cembroides* iWUE (Figure 6). This result, combined with the decreasing trend of growth (BAI, Figure 2), could indicate a low photosynthetic activity triggered by a greater plasticity of stomatal regulation for this pine. Similar results have been reported for a dry area of the Mediterranean (Altieri et al., 2015), where the species with a tighter stomatal regulation also presented higher iWUE. Unexpectedly, *P. engelmannii* had just slightly higher values of iWUE than *A. durangensis*, which reinforces the possibility that in a warmer and drier future climate, *P. cembroides* can outcompete *P. engelmannii* at dry sites, whereas the latter species could expand toward wet

sites located at higher elevation where *A. durangensis* grows nowadays but could experience drought-triggered dieback in the future.

CONCLUSIONS

Matching tree-ring, wood anatomical and isotope analysis resulted in an efficient combination of methodologies that provided better insight on species-specific responses of three conifers and how they may adapt to climate change. *P. cembroides*, with a very distinct wood anatomical traits (smaller cells), a compact morphology (smaller trees with close-packed crowns) and an extremely high iWUE, stands as the species better adapted to its current environment and could be less affected by a future warmer and drier climate. On the other hand, it shows the lowest growth rates with a decreasing tendency over the last 30 years. *P. engelmannii* and *A. durangensis* show high plasticity at a wood anatomical level for a prompt response to seasonal water availability, but this plasticity likely gives no advantages under a climate with longer and more frequent drought spells (see Figure S5).

These findings provide a better understanding of the ecological mechanisms developed by the studied conifer species in northern Mexico. However, further research, including xylogenesis analysis and monitoring of the different populations of these tree species, would be still necessary to reach a clearer understanding of their future responses to weather patterns. Our multi-proxy approach could be used in other forests to characterize the in situ functioning of trees, e.g. growth, water use, and development of strategies for forest management under these new climate change scenarios.

ACKNOWLEDGMENTS

We are very grateful to Maria Elena Gelain, Department of Comparative Biomedicine and Food Science, University of Padua, for allowing us access to the D-sight 2.0 System automatic scanner (Grandi Attrezzature fund, University of Padua). Funding was provided by Mexican CONACYT (CB-2013/222522-A1-S-21471) and COCYTED (FOMIX-2017) projects also by the Spanish Ministry of Economy project (Fundiver, CGL2015-69186-C2-1-R) and (MINECO/FEDER grant number AGL2015-68274-C3-3-R). We also thank PIDCAF-UJED, DendroRed (https://dendrored.ujed.mx).

CONFLICT OF INTEREST

None declared.

REFERENCES

Adams, H.D., Kolb, T.E., 2005. Tree growth response to drought and temperature in a mountain landscape in northern Arizona, USA. J. Biogeogr. doi:10.1111/j.1365-2699.2005.01292.x

Aguirre, O., Hui, G., Von Gadow, K., Jiménez, J., 2003. An analysis of spatial forest structure using neighbourhood-based variables. For. Ecol. Manage. 183, 137–145. doi:10.1016/S0378-1127(03)00102-6

Altieri, S., Mereu, S., Cherubini, P., Castaldi, S., Sirignano, C., Lubritto, C., Battipaglia, G., 2015. Tree-ring carbon and oxygen isotopes indicate different water use strategies in three Mediterranean shrubs at Capo Caccia (Sardinia , Italy). Trees 29, 1593–1603. doi:10.1007/s00468-015-1242-z

Barbour, M.M., 2007. Stable oxygen isotope composition of plant tissue: a review. Funct. Plant Biol. 34, 83–94. doi:10.1071/FP06228

Battipaglia G, Campelo F, Vieira J, Grabner M, De Micco V, Nabais C, Di Filippo A. 2016.

Structure and function of intra-annual density fluctuations: mind the gaps. Front. Plant Sci.7: 595. https://doi.org/10.3389/fpls.2016.00595.

Battipaglia G, De Micco V, Brand WA, Linke P, Aronne G, Saurer M, Cherubini P. 2010. Variations of vessel diameter and δ13C in false rings of Arbutus unedo L. reflect different environmental conditions. New Phytol. 188: 1099–1112. doi: 10.1111/j.1469-8137.2010.03443.x.

Bennett, A.C., Mcdowell, N.G., Allen, C.D., Anderson-Teixeira, K.J., 2015. Larger trees suffer most during drought in forests worldwide. Nat. Plants. doi:10.1038/nplants.2015.139

Bickford, I.N., Fulé, P.Z., Kolb, T.E., 2011. Growth Sensitivity to Drought of Co-Occurring Pinus spp. along an Elevation Gradient in Northern Mexico. West. North Am. Nat. 71, 338–348. doi:10.3398/064.071.0302

Bouriaud, O., Leban, J.-M., Bert, D., Deleuze, C., 2005. Intra-annual variations in climate influence growth and wood density of Norway spruce. Tree Physiol. 25, 651–660. doi:10.1093/treephys/25.6.651

Brendel, O., Iannetta, P.P.M., Stewart, D., 2000. A rapid and simple method to isolate pure alpha-cellulose. Phytochem. Anal. 11, 7–10. doi:10.1002/(SICI)1099-1565(200001/02)11:1<7::AID-PCA488>3.0.CO;2-U

Campelo, F., Nabais, C., Freitas, H., Gutiérrez, E., 2007. Climatic significance of tree-ring width and intra-annual density fluctuations in Pinus pinea from a dry Mediterranean area in Portugal. Ann. For. Sci. 64, 229–238. doi:10.1051/forest:2006107

Canadell, J., Zedler, P.H., 1995. Underground Structures of Woody Plants in Mediterranean Ecosystems of Australia, California, and Chile, in: Fox, M., Kalin, M., Zedler, P. (Eds.),

608 Ecology and Biogeography of Mediterranean Ecosystems in Chile, California and
609 Australia. pp. 177–210. doi:10.1007/978-1-4612-2490-7_8

610 Carrer, M., von Arx, G., Castagneri, D., Petit, G., 2015. Distilling allometric and
611 environmental information from time series of conduit size: the standardization issue
612 and its relationship to tree hydraulic architecture. Tree Physiol. 35, 27–33.
613 doi:10.1093/treephys/tpu108

614 Castagneri, D., Battipaglia, G., von Arx, G., Pacheco, A., Carrer, M., 2018. Tree-ring
615 anatomy and carbon isotope ratio show both direct and legacy effects of climate on
616 bimodal xylem formation in Pinus pinea. Tree Physiol. 38, 1098–1109.
617 doi:10.1093/treephys/tpy036

618 Castagneri, D., Fonti, P., Von Arx, G., Carrer, M., 2017. How does climate influence xylem
619 morphogenesis over the growing season? Insights from long-Term intra-ring anatomy in
620 Picea abies. Ann. Bot. 119, 1011–1020. doi:10.1093/aob/mcw274

621 Constante García, V., Villanueva Díaz, J., Cerano Paredes, J., Cornejo Oviedo, E.H.,
622 Valencia Manzo, S., 2009. Dendrocronología de Pinus cembroides Zucc. Y
623 Reconstrucción de Precipitación, estacional para el sureste de Coahuila. Rev. Cienc. For.
624 en México 34, 17–39.

625 Cook, B.I., Seager, R., 2013. The response of the North American Monsoon to increased
626 greenhouse gas forcing. J. Geophys. Res. Atmos. doi:10.1002/jgrd.50111

627 Cook, E.R., 1985. A Time Series Analysis Approach to Tree Ring Standardization. Sch.
628 Renew. Nat. Resour. Arizona University, Tucson, USA.

629 Cook, E.R., Briffa, K., Shiyatov, S., Mazepa, V., 1990. Tree-ring standardization and growth-
630 trend estimation, in: E. R. Cook and L. A. Kairiukstis (Ed.), Methods of
631 Dendrochronology: Applications in the Environmental Sciences. Kluwer Academic
632 Publisher, Dordrecht, The Netherlands, pp. 104–123.

633 De Micco, V., Campelo, F., De Luis, M., Br??uning, A., Grabner, M., Battipaglia, G.,
634 Cherubini, P., 2016. Intra-annual density fluctuations in tree rings: How, when, where,
635 and why? IAWA J. 37, 232–259. doi:10.1163/22941932-20160132

636 De Micco, V., Carrer, M., Rathgeber, C.B.K., Julio Camarero, J., Voltas, J., Cherubini, P.,
637 Battipaglia, G., 2019. From xylogenesis to tree rings: Wood traits to investigate tree
638 response to environmental changes. IAWA J. 42. doi:10.1163/22941932-40190246

639 Farquhar, G.D., O'Leary, H.M., Berry, J.A., 1982. On the relationship between carbon
640 isotope discrimination and the intercellular carbon dioxide concentration in leaves. Aust.
641 J. Plant Physiol. 9, 121–137.

642 Farquhar, G.D., Richards, R.A., 1984. Isotopic composition of plant carbon correlates with
643 water-use efficiency of wheat genotypes. Aust. J. Plant Physiol. 11, 539–552.

644 Fonti, P., Von Arx, G., García-González, I., Eilmann, B., Sass-Klaassen, U., Gärtner, H.,
645 Eckstein, D., 2010. Studying global change through investigation of the plastic
646 responses of xylem anatomy in tree rings. New Phytol. 185, 42–53. doi:10.1111/j.1469-
647 8137.2009.03030.x

648 Fritts, H.C., 1976. Tree Rings and Climate. Elsevier, Caldwell, NJ, USA. doi:10.1016/B978-
649 0-12-268450-0.X5001-0

650 Fritts, H.C., 1974. Relationships of Ring Widths in Arid-Site Conifers to Variations in
651 Monthly Temperature and Precipitation. Ecol. Monogr. doi:10.2307/1942448

652 Fulé, P.Z., Ramos-Gómez, M., Cortés-Montaño, C., Miller, A.M., 2011. Fire regime in a
653 Mexican forest under indigenous resource management. Ecol. Appl. 21, 764–775.
654 doi:10.1890/10-0523.1

655 Gaudinski, J.B., Dawson, T.E., Quideau, S., Schuur, E.A.G., Roden, J.S., Trumbore, S.E.,
656 Sandquist, D.R., Oh, S.-W., Wasylishen, R.E., 2005. Comparative Analysis of Cellulose
657 Preparation Techniques for Use with 13 C, 14 C, and 18 O Isotopic Measurements.
658 Anal. Chem. 77, 7212–7224. doi:10.1021/ac050548u

659 Gernandt, D.S., la Rosa, J.A.P.-D., 2014. Biodiversity of Pinophyta (conifers) in Mexico.
660 Rev. Mex. Biodivers. doi:10.7550/rmb.32195

661 González-Cásares, M., Pompa-García, M., Camarero, J.J., 2017. Differences in climate–
662 growth relationship indicate diverse drought tolerances among five pine species
663 coexisting in Northwestern Mexico. Trees - Struct. Funct. doi:10.1007/s00468-016-
664 1488-0

665 González-Elizondo, M.S., González-Elizondo, M., Tena-Flores, J.A., Ruacho-González, L.,
666 López-Enríquez, I.L., 2012. Vegetación de la sierra madre occidental, México: Una
667 síntesis. Acta Bot. Mex. doi:https://doi.org/10.21829/abm100.2012.40

668 Granda, E., Rossatto, D.R., Camarero, J.J., Voltas, J., Valladares, F., 2014. Growth and
669 carbon isotopes of Mediterranean trees reveal contrasting responses to increased carbon
670 dioxide and drought. Oecologia 174, 307–317. doi:10.1007/s00442-013-2742-4

671 Gutiérrez-García, J. V, Rodríguez-Trejo, D.A., Villanueva-Morales, A., García-Díaz, S.,
672 Romo-Lozano, J.L., 2015. Calidad del agua en la producción de Pinus cembroides Zucc.
673 en vivero. Agrociencia 205–219.

674 Hacke, U.G., Sperry, J.S., Pockman, W.T., Davis, S.D., McCulloh, K.A., 2001. Trends in
675 wood density and structure are linked to prevention of xylem implosion by negative
676 pressure. Oecologia 126, 457–461. doi:10.1007/s004420100628

677 Herrera-soto, G., Gonz, M., 2018. Growth of *Pinus cembroides* Zucc . in Response to
678 Hydroclimatic Variability in Four Sites Forming the Species Latitudinal and
679 Longitudinal Distribution Limits. doi:10.3390/f9070440

680 Holmes, R.L., 1983. Computer-assisted quality control in tree-ring dating and measurement.
681 Tree-Ring Bull 43, 68–78.

682 IPCC Working Group 1, I., Stocker, T.F., Qin, D., Plattner, G.-K., Tignor, M., Allen, S.K.,
683 Boschung, J., Nauels, A., Xia, Y., Bex, V., Midgley, P.M., 2013. IPCC, 2013: Climate
684 Change 2013: The Physical Science Basis. Contribution of Working Group I to the Fifth
685 Assessment Report of the Intergovernmental Panel on Climate Change. IPCC AR5,
686 1535.

687 Kelly, A.E., Goulden, M.L., 2008. Rapid shifts in plant distribution with recent climate
688 change. Proc. Natl. Acad. Sci. doi:10.1073/pnas.0802891105

689 Linares, J.C., Camarero, J.J., Carreira, J.A., 2010. Competition modulates the adaptation
690 capacity of forests to climatic stress: Insights from recent growth decline and death in
691 relict stands of the Mediterranean fir Abies pinsapo. J. Ecol. doi:10.1111/j.1365-
692 2745.2010.01645.x

McCarroll, D., Loader, N.J., 2004. Stable isotopes in tree rings. Quat. Sci. Rev. 23, 771–801. doi:10.1016/j.quascirev.2003.06.017

McDowell, N.G., Allen, C.D., Marshall, L., 2010. Growth, carbon-isotope discrimination, and drought-associated mortality across a Pinus ponderosa elevational transect. Glob. Chang. Biol. doi:10.1111/j.1365-2486.2009.01994.x

Moreno-Gutiérrez, C., Battipaglia, G., Cherubini, P., Delgado Huertas, A., Querejeta, J.I., 2015. Pine afforestation decreases the long-term performance of understorey shrubs in a semi-arid Mediterranean ecosystem: a stable isotope approach. Funct. Ecol. 29, 15–25. doi:10.1111/1365-2435.12311

Moreno-Gutiérrez, C., Dawson, T.E., Nicolás, E., Querejeta, J.I., 2012. Isotopes reveal contrasting water use strategies among coexisting plant species in a mediterranean ecosystem. New Phytol. doi:10.1111/j.1469-8137.2012.04276.x

Novak, K., Čufar, K., de Luis, M., Sánchez, M.A.S., Raventós, J., 2013. Age, climate and intra-annual density fluctuations in Pinus halepensis in Spain. IAWA J. 34, 459–474. doi:10.1163/22941932-00000037

Pacheco, A., Camarero, J.J., Carrer, M., 2016. Linking wood anatomy and xylogenesis allows pinpointing of climate and drought influences on growth of coexisting conifers in continental Mediterranean climate. Tree Physiol. 36. doi:10.1093/treephys/tpv125

Pacheco, A., Camarero, J.J., Ribas, M., Gazol, A., Gutierrez, E., Carrer, M., 2018. Disentangling the climate-driven bimodal growth pattern in coastal and continental Mediterranean pine stands. Sci. Total Environ. 615, 1518–1526. doi:10.1016/j.scitotenv.2017.09.133

Pittermann, J., Sperry, J.S., Wheeler, J.K., Hacke, U.G., Sikkema, E.H., 2006. Mechanical reinforcement of tracheids compromises the hydraulic efficiency of conifer xylem. Plant, Cell Environ. doi:10.1111/j.1365-3040.2006.01539.x

Pompa-García, M., González-Cásares, M., Acosta-Hernández, A.C., Camarero, J.J., Rodríguez-Catón, M., 2017a. Drought influence over radial growth of Mexican conifers inhabiting mesic and xeric sites. Forests 8, 1–13. doi:10.3390/f8050175

Pompa-García, M., Sánchez-Salguero, R., Camarero, J.J., 2017b. Observed and projected impacts of climate on radial growth of three endangered conifers in northern Mexico indicate high vulnerability of drought-sensitive species from mesic habitats. Dendrochronologia 45, 145–155. doi:10.1016/j.dendro.2017.08.006

Porté, A., Loustau, D., 2001. Seasonal and interannual variations in carbon isotope discrimination in a maritime pine (Pinus pinaster) stand assessed from the isotopic composition of cellulose in annual rings, in: Tree Physiology. doi:10.1093/treephys/21.12-13.861

Salzer, M.W., Kipfmueller, K.F., 2005. Reconstructed temperature and precipitation on a millennial timescale from tree-rings in the southern Colorado Plateau, U.S.A. Clim. Change. doi:10.1007/s10584-005-5922-3

Sánchez-González, A., 2008. Una visión actual de la diversidad y distribución de los pinos de México. Madera y Bosques. doi:10.1016/B978-0-08-044666-0.50026-9

Saurer, M., Borella, S., Leuenberger, M., 1997. □18O of tree rings of beech (Fagus sylvatica) as a record of □18O of the growing season precipitation. Tellus, Ser. B Chem. Phys.

736 Meteorol. 49, 80–92.

737 Saurer, M., Siegwolf, R.T.W., Schweingruber, F.H., 2004. Carbon isotope discrimination
738 indicates improving water-use efficiency of trees in northern Eurasia over the last 100
739 years. Glob. Chang. Biol. doi:10.1111/j.1365-2486.2004.00869.x

740 Seibt, U., Rajabi, A., Griffiths, H., Berry, J.A., 2008. Carbon isotopes and water use
741 efficiency: Sense and sensitivity. Oecologia 155, 441–454. doi:10.1007/s00442-007-
742 0932-7

743 Shestakova, T.A., Camarero, J.J., Ferrio, J.P., Knorre, A.A., Gutiérrez, E., Voltas, J., 2017.
744 Increasing drought effects on five European pines modulate Δ13C-growth coupling
745 along a Mediterranean altitudinal gradient. Funct. Ecol. 31, 1359–1370.
746 doi:10.1111/1365-2435.12857

747 Singer, M.B., Stella, J.C., Dufour, S., Piégay, H., Wilson, R.J.S., Johnstone, L., 2013.
748 Contrasting water-uptake and growth responses to drought in co-occurring riparian tree
749 species. Ecohydrology. doi:10.1002/eco.1283

750 Stahle, D.W., Cook, E.R., Burnette, D.J., Villanueva, J., Cerano, J., Burns, J.N., Grif, D.,
751 Cook, B.I., Acu, R., Torbenson, M.C.A., Szejner, P., Howard, I.M., 2016. The Mexican
752 Drought Atlas : Tree-ring reconstructions of the soil moisture balance during the late
753 pre-Hispanic , colonial , and modern eras 149, 34–60.
754 doi:10.1016/j.quascirev.2016.06.018

755 V. Masson-Delmotte, P. Zhai, H. O. Pörtner, D. Roberts, J. Skea, P.R. Shukla, A. Pirani, W.
756 Moufouma-Okia, C. Péan, R. Pidcock, S. Connors, J. B. R. Matthews, Y. Chen, X.
757 Zhou, M. I. Gomis, E. Lonnoy, T. Maycock, M. Tignor, T.W., 2018. IPCC, 2018:
758 Summary for Policymakers. In: Global warming of 1.5°C. Geneve.

759 Van de Water, P.K., Leavitt, S.W., Betancourt, J.L., 2002. Leaf δ13C variability with
760 elevation, slope aspect, and precipitation in the southwest United States. Oecologia.
761 doi:10.1007/s00442-002-0973-x

762 Vicente-Serrano S.M., Beguería, S., López-Moreno, J.I., 2010. A Multi-scalar drought index
763 sensitive to global warming: The Standardized Precipitation Evapotranspiration Index -
764 SPEI. J. Clim. 23: 1696–1718.

765 Vicente-Serrano, S.M., Gouveia, C., Camarero, J.J., Begueria, S., Trigo, R., Lopez-Moreno,
766 J.I., Azorin-Molina, C., Pasho, E., Lorenzo-Lacruz, J., Revuelto, J., Moran-Tejeda, E.,
767 Sanchez-Lorenzo, A., 2013. Response of vegetation to drought time-scales across global
768 land biomes. Proc. Natl. Acad. Sci. 110, 52–57. doi:10.1073/pnas.1207068110

769 Villanueva-Díaz, J., Cerano-Paredes, J., Rosales Mata, S., Arrocena López, J.C., Stahle,
770 D.W., Ruiz Corral, J.A., Martinez-Sifuentes, A.R., 2014. Variabilidad hidroclimática
771 reconstruida con anillos de árboles para la cuenca alta del Río Mezquital, Durango. Rev.
772 Mex. Ciencias Agrícolas 1897–1912.

773 Villanueva-Diaz, J., Stahle, D.W., Luckman, B.H., Cerano-Paredes, J., Therrell, M.D.,
774 Cleaveland, M.K., Cornejo-Oviedo, E., 2007. Winter-spring precipitation
775 reconstructions from tree rings for northeast Mexico. Clim. Change.
776 doi:10.1007/s10584-006-9144-0

777 von Arx, G., Carrer, M., 2014. ROXAS – A new tool to build centuries-long tracheid-lumen
778 chronologies in conifers. Dendrochronologia 32, 290–293.

779 doi:10.1016/j.dendro.2013.12.001

780 Williams, A.P., Allen, C.D., Macalady, A.K., Griffin, D., Woodhouse, C.A., Meko, D.M.,
781 Swetnam, T.W., Rauscher, S.A., Seager, R., Grissino-Mayer, H.D., Dean, J.S., Cook,
782 E.R., Gangodagamage, C., Cai, M., Mcdowell, N.G., 2013. Temperature as a potent
783 driver of regional forest drought stress and tree mortality. Nat. Clim. Chang.
784 doi:10.1038/nclimate1693

785 Willson, C.J., Manos, P.S., Jackson, R.B., 2008. Hydraulic traits are influenced by
786 phylogenetic history in the drought-resistant, invasive genus Juniperus (Cupressaceae).
787 Am. J. Bot. 95, 299–314. doi:10.3732/ajb.95.3.299

788

789

SUPPLEMENTARY INFORMATION

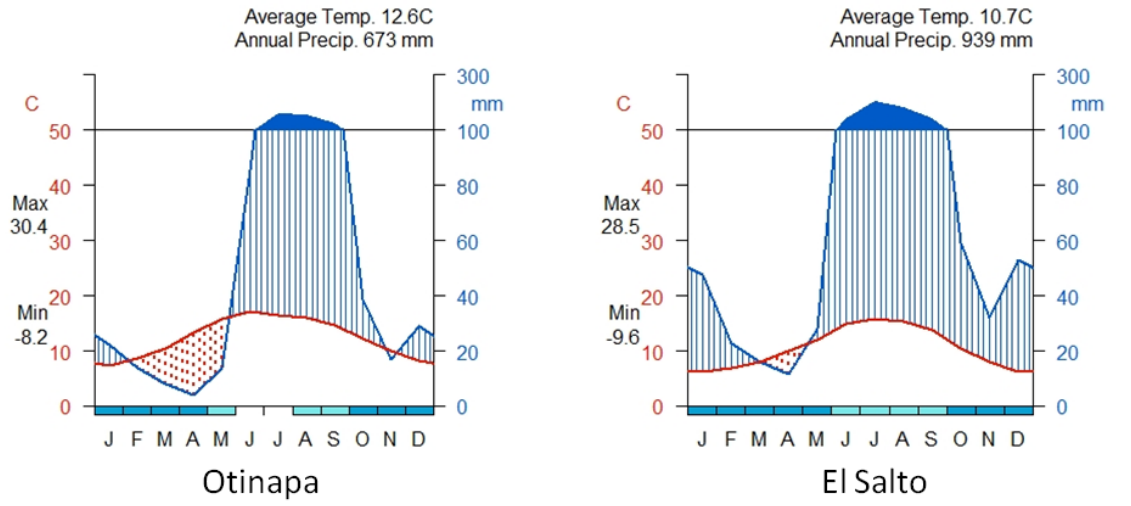

Figure S1. Climate diagrams of the climate stations from the dry (Otinapa, 1962-2015 data) and wet (El Salto, 1946-2015 data) study sites.

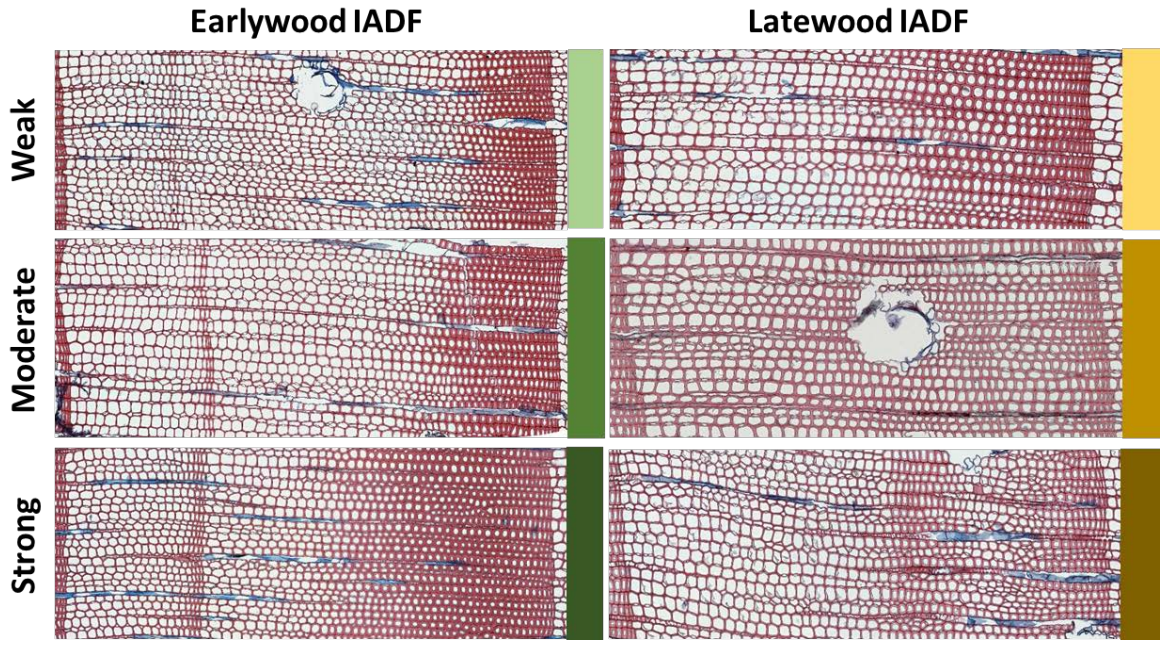

Figure S2: Visual aid for the qualitative characterization of intra-annual density fluctuations (IADF) using three level scale of intensity (weak, moderate and strong) and separated in IADFs occurring within the earlywood (producing latewood-like cells) and latewood (producing earlywood-like cells). The color scale of intensity correspond to the one used on Figure 3.

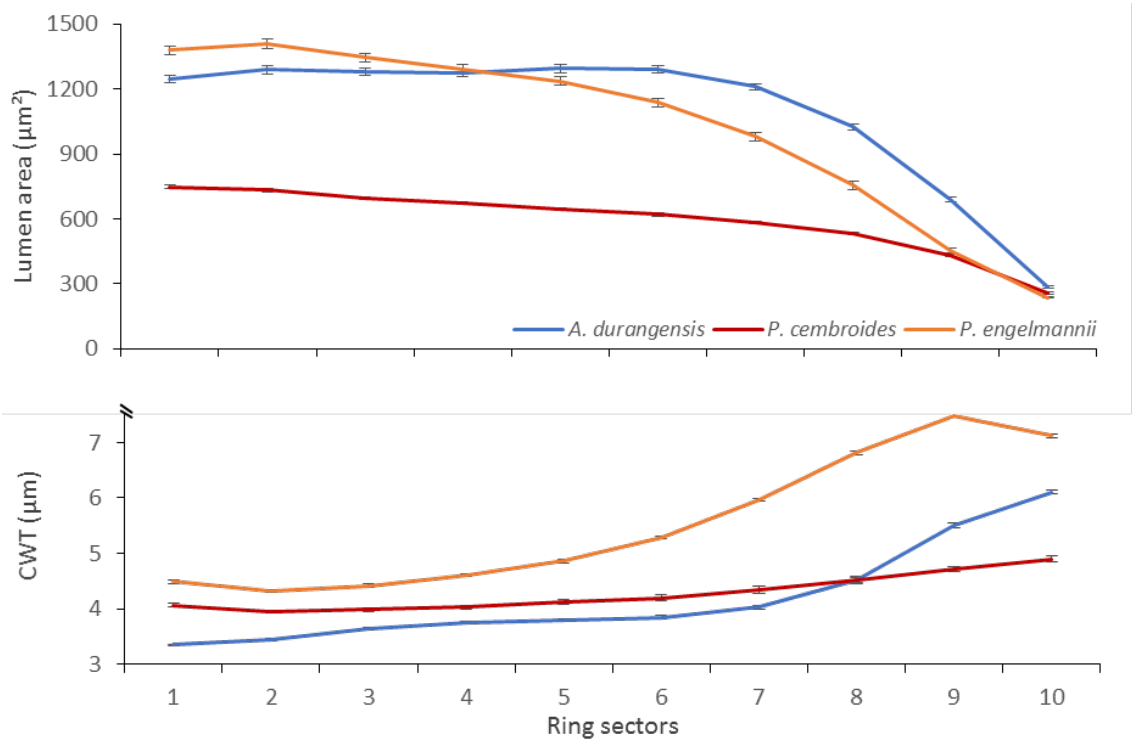

Figure S3. Intra-annual values (means ± SE) of lumen area and cell-wall thickness (CWT) of the three studied conifer species (wet site, *Abies durangensis*; dry site, *Pinus cembroides* and *Pinus engelmannii*). Values are shown for the common period (1950- 2014).

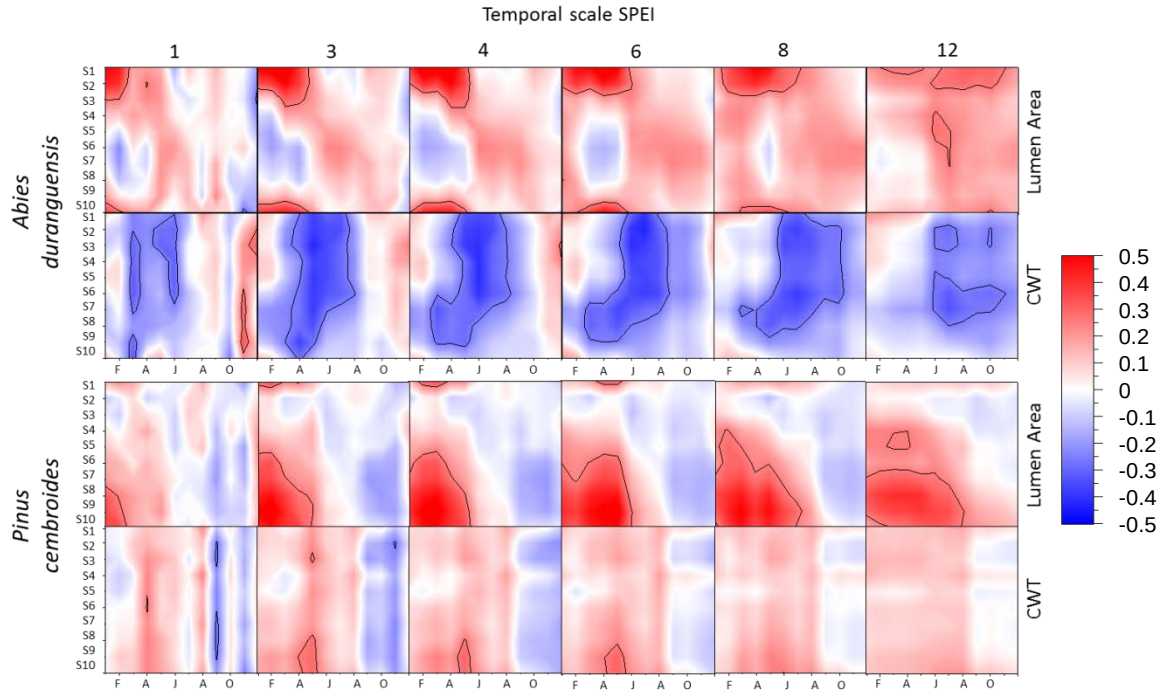

Figure S4. Pearson correlations calculated between the Standardized Precipitation Evapotranspiration Index (SPEI) drought index and sectorized anatomical traits (lumen area; CWT, cell-wall thickness) for two of the three studied conifer species (wet site, *Abies durangensis*; dry site, *Pinus cembroides*). The Y axes correspond to ten tree-ring radial sectors from the early earlywood (S1) to the late latewood (S10). The SPEI was calculated on scales of 1, 3, 4, 6, 8 and 12-month long (columns) from January–December. The graphs show the Pearson correlation coefficients (*r*) using color scales. Correlation values above $|0.232|$ are significant ($P < 0.05$) and shown by the black contour line. *Pinus engelmannii* did not present significant correlations, thus was not included in the figure.

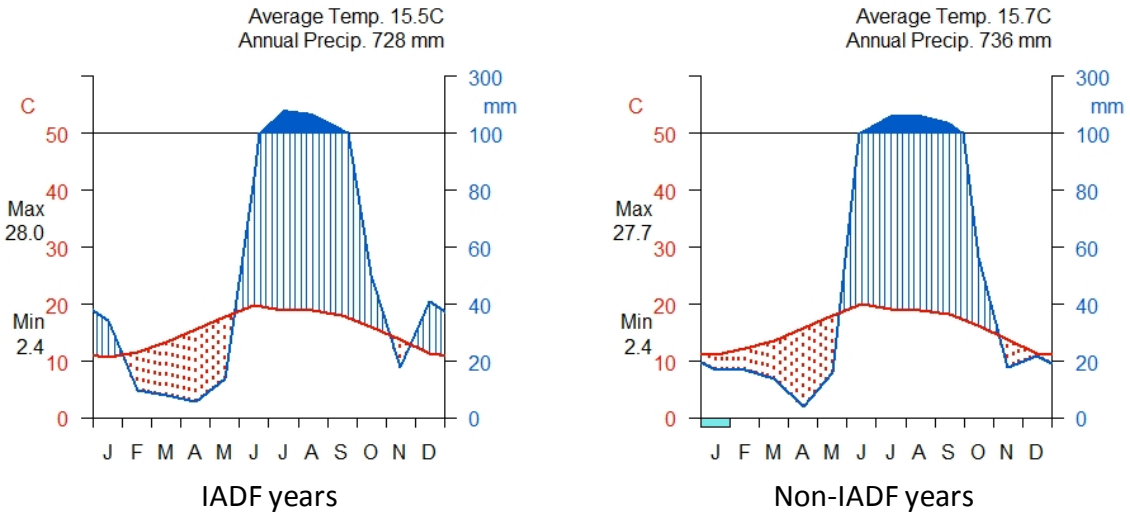

Figure S5. Climate diagrams from CRU (0.5º-gridded) climate data covering both the study wet and dry sites and splitting the years with high (+50%, left plot) and low (-50%, right plot) frequency of intra-annual density fluctuations (IADF).